Journal of Physics and Chemistry of Solids 75 (2014) 670–679

Contents lists available at ScienceDirect

Journal of Physics and Chemistry of Solids

journal homepage: www.elsevier.com/locate/jpcs

Anticrossing spectroscopy in multi-nanolayer structures

Vladimir I. Makarov [a,*], Igor Khmelinskii [b]

[a] Department of Physics, University of Puerto Rico, Rio Piedras, P.O. Box 23343, San Juan, PR 00931-3343, USA
[b] Universidade do Algarve, FCT, DQF, and CIQA, P8005-139 Faro, Portugal

ARTICLE INFO

Article history:
Received 14 October 2013
Received in revised form
24 January 2014
Accepted 25 January 2014
Available online 4 February 2014

Keywords:
A. Interfaces
B. Magnetic materials
C. Semiconductor
D. Magnetic properties
E. Spin-density waves

ABSTRACT

Presently we explored nanosandwich structures with graphite (Gt) and graphene (Gn) nanolayers. We found that in Pt–SiO_2–Gt, Pt–BN–Gt and Pt–SiO_2–Ni–Gn structures the spectra may be decomposed into several components, each corresponding to a different value of the total spin angular momentum *S*. Only one component was required to describe the Pt–SiO_2–Ni–Gn spectra at 5.3 K, with additional components appearing at higher temperatures. On the other hand, a single component described the Pt–BN–Ni–Gn spectra at all temperatures. Temperature dependence of the spectra of the Pt–SiO_2–Ni–Gn system was studied in the 5.3–75.3 K range. Presently we obtained experimental results for novel sandwich systems, with the Gn layer only two monoatomic layers thick. Thus, we compared experimental spectra of a three-nanolayer sandwich system containing a Gt nanolayer with those of a four-nanolayer system containing a diatomic Gn layer. The experimental results were discussed using a theoretical model of the respective physical mechanisms. We propose an exchange anticrossing mechanism, whereby the spin-state polarization of the given Zeeman's substate in the Pt nanolayer is transported to Gt or Ni–Gn nanolayer by the exchange interaction between the two layers. As long as exchange interaction coupling spin states in different nanolayers is involved, we term the respective spectra the "spin anticrossing exchange-resonance spectra". This clarifies the physical origins of some of the model parameters, i.e. the growing external magnetic field shifts the Zeeman's substates in the different layers differently, producing the anticrossing spectrum. In the frameworks of the developed model, we propose spin–orbit (SO) interaction as the main factor inducing the spin–lattice relaxation, which is one of the important factors determining the line shape. We performed *ab initio* calculations of the SO interaction in carbon and metal nanolayers, finding that the SO interactions monotonously increase with the atomic number.

Published by Elsevier Ltd.

1. Introduction

Spintronics involve active manipulation of spin degrees of freedom in solid-state systems. The control of spin is then a control of either population and phase of spins in an ensemble of particles, or a coherent spin manipulation in single- or multiple-spin systems. The goals of spintronics are to study interactions between spin and its solid-state environment and produce useful spintronic devices. Thus fundamental studies focus on spin transport, dynamics and relaxation.

One of the most important problems in spintronics is generation of spin-polarized states, usually by creating a nonequilibrium spin population. Spin can be oriented using optical techniques by transferring angular momenta of circularly-polarized photons to electrons, although electrical spin injection is more desirable for practical applications. However, the rates of spin accumulation depend on spin relaxation rates, in both cases. The mechanisms of spin relaxation have been analyzed earlier [1–8]. Typical spin relaxation time scales are in the pico- to microsecond time range. Spin detection is also important. The common goal in many spintronic devices is to maximize the spin-polarized state generation and detection sensitivity. Earlier we proposed a novel device to generate and detect spin-polarized states [4–8], using exchange state-anticrossing phenomenon.

State anticrossing is quite well known in quantum physics, investigated for example in intermediate-case molecules [1–3]. Earlier we reported on spin-polarized state transport between two conductive nanolayers, separated by an insulator [4–8], interpreted as resulting from the exchange anticrossing resonance. Phenomenological models were proposed and validated [4–8], without discussing the underlying physical mechanisms in detail.

The results in three-nanolayer metal-dielectric-semiconductor (MDS) devices were interpreted using phenomenological models and *ab initio* quantum chemical calculations [8]. We found that the

* Corresponding author. Tel.: +1 787 529 2010; fax: 1 787 756 7717.
E-mail addresses: vmvimakarov@gmail.com, vladimir.makarov@upprrp.edu (V.I. Makarov).

http://dx.doi.org/10.1016/j.jpcs.2014.01.022
0022-3697 Published by Elsevier Ltd.

accuracy of the *ab initio* methods is sufficient, being able to reproduce the structure of exchange anticrossing resonance spectra. The *ab initio* calculations acceptably reproduce the spectral line positions and numbers in the experimental spectra, with encouraging prospects for future usage of this theoretical approach.

Ferromagnetism in different semiconductor–transition metal systems is a very interesting phenomenon, which may find spintronic applications. This phenomenon, however, has not been explored either experimentally or theoretically in nanolayers. Note that according to *ab initio* analysis at high temperatures, ferromagnetism was predicted to occur in GaN doped with transition metals. Theoretically, such materials can lead to semiconductor-based spintronic applications [9–11]. Spintronic devices have more functionality in comparison with conventional semiconductors, using both electrical charge and spin of the electrons. Ferromagnetism in semiconductors diluted by atoms of transition elements at room temperature was reported earlier [12]. Magnetic doping is usually limited by solubility of transition metals in semiconductors, as was the case of GaN doped by Mn [13,14]. Ferromagnetism may be obtained with 3d and some 4d non-magnetic dopants [15–17]. For example, properties of Ag and Cd dopants in ZnO have been considered theoretically earlier [18,19]. It has also been shown that Pd atoms in GaN are ferromagnetically ordered [20,21].

In the present study, we focus our attention on detailed experimental investigation of three- and four-nanolayer Pt–SiO_2–graphite (PSGt), Pt–SiO_2–Ni–graphene (PSNGn), Pt–BN nanomesh–graphite (PBGt) and Pt–BN nanomesh–Ni–graphene (PBNGn) devices. All of these devices were experimentally tested for spin-polarized state transport from the Pt nanolayer to Gt or Ni–Gn nanolayer, obtaining experimental data on the effects of diatomic graphene layers on spin transport.

Our goals include recording of the exchange anticrossing resonance spectra for the new devices, where the metal or semiconductor nanolayer in the output section of the device was substituted by either Gt or Gn. Another important goal is to continue development of the theory of exchange anticrossing resonances observed in nanolayer sandwich devices, along with analysis of the physical mechanisms behind the earlier introduced phenomenological models [4–8]. The developed theoretic approach was used to interpret, analyze and simulate the experimentally recorded spectra, advancing the main goal of the present studies.

2. Experimental

The presently used experimental setup has been described in detail earlier [4–7]. In short, it included a home-made device, built around a solid-state sandwich structure, deposited on a (100) Si substrate (commercial product, 0.15 mm thickness). A partial cross-section of a typical sandwich structure has been published earlier [4,5]. Charge sputtering was used to deposit the metal layers, and laser vapor deposition was used to deposit the dielectric layer. Graphite and graphene layers were deposited in a tube-furnace reactor [22–25]. In particular, graphite nanolayer of controllable thickness was deposited on top of the SiO_2 nanolayer of the previously prepared Si–Pt–SiO_2 sandwich. The temperature in the tube-furnace reactor was increased from 25 °C to 950 °C at 10^{-3} Torr; next an H_2+5% CH_4 gas mixture was passed through the reactor at 200 Torr total pressure and 100 ccm gas flow during a certain time, providing layer growth at about 1.3 nm/min rate, for at least 5 min. A typical Raman spectrum of the deposited graphite nanolayer is shown in Fig. 1. Raman spectra were recorded using a home-made Raman spectrometer assembled

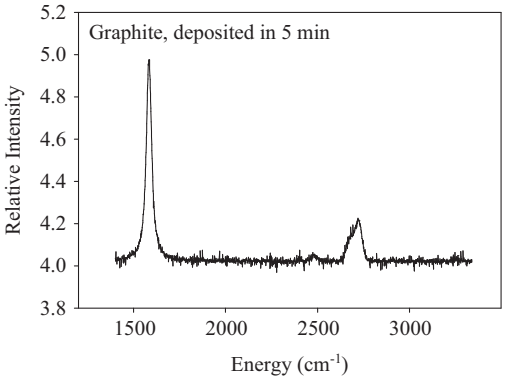

Fig. 1. Raman spectrum of the graphite nanolayer deposited in 5 min on top of the SiO_2 nanolayer.

from commercial components as described in [26], with the Ar ion laser operating at 514.5 nm used as the radiation source.

Graphene was deposited on SiO_2 with an intermediate Ni catalyst nanolayer 8.7 nm thick using the method proposed earlier [27]. Raman spectrum of the deposited material is shown in Fig. 2.

Note that the recorded spectrum corresponds with good accuracy to that of a graphene bilayer [28].

The two devices of Pt–BN–Gt and Pt–BN–Ni–Gn compositions were produced using the same methods. The BN-nanomesh layer was deposited on top of the Pt layer using Pulsed Laser Deposition. A solid BN target was evaporated by KrF excimer laser pulses (Lambda Physics, LPX-200) at $\sim 10^{-7}$ Torr, covering the Si–Pt target. The average pulse energy and repetition rate were was 370 mJ/pulse and 10 Hz, respectively. Typical Raman spectrum of the deposited BN nanomesh is shown in Fig. 3. The Raman spectrum reveals two characteristic bands at 803 and 1356 cm^{-1}, typical for hexagonal nanostructured BN. The A_{2u} (805 cm^{-1}) mode is close to 803 cm^{-1} and the E_{1v} (1367 cm^{-1}) mode is close to 1356 cm^{-1} mode of the bulk material [29–33].

The layer thickness was verified by transmission electron microscopy (TEM) on cross-cut samples, prepared using heavy-ion milling.

The device included a ferrite needle (TPS&TPSA, Power Electronics Technology), with the needle tip 50 μm in diameter, made of a stainless steel capillary filled by ferrite powder suspended in glycerol, and the body 1 mm in diameter. A spiral coil of copper wire (0.3 mm wire diameter, 10 turns) was wound on the needle body. The needle tip touched the surface of a Si substrate at the (100) plane. A second ferrite item (TPS&TPSA, Power Electronics Technology), with the input surface 10 mm in diameter and the body 1 mm in diameter, contacted the output metal surface by way of a magnetic contact provided by ferrite powder suspended in glycerol (1:1 w/w) (TPS&TPSA, Power Electronics Technology, 25 μm average particle diameter). Copper wire, 0.3 mm in diameter, was wound on the body of the item (10 turns). Note that the same high-frequency ferrite material was used everywhere, rated for up to 100 MHz applications. The entire assembly with the nanosandwich sample was placed into a liquid nitrogen bath ($T \approx 77$ K), to reduce noise.

A home-made current generator, with the electronic circuit shown in Fig. 1(b), was controlled via an I/O data acquisition board (National Instruments DAQ, PCI-6034E), which was programmed in the LABVIEW environment and run on a Dell PC. The generator fed pulsed output currents of up to 10 A into the input coil. The pulse shape was programmed to reproduce the linear function,

$$I_2(t) = \begin{cases} 0, & 0 \le t < t_0 \\ I_0(t - t_{\epsilon 0})/\tau, & t_0 \le t < t_0 + \tau \\ 0, & t_0 + \tau \le t \end{cases} \quad (1)$$